Available on CMS information server **CMS CR 2006/067**

CMS Conference Report

August 2006

Test beam results on the performance of the CMS electromagnetic calorimeter

Alexandre Zabi
Imperial College, London, UK.
On behalf of the CMS ECAL group

Abstract

The performance of the CMS electromagnetic calorimeter has been studied with the test beam data recorded with a fully equipped barrel supermodule. An efficient method for signal amplitude reconstruction has been implemented and tested on these data. Results on energy resolution and electronics noise show excellent performance of the apparatus. Effects attributed to shower containment in crystal arrays were investigated and a set of corrections has been formulated and used to provide results on energy resolution.

Presented at:
XII International conference on calorimetry in high energy physics, June 5-9 2006, Chicago, USA.

1 Introduction

1.1 CMS electromagnetic calorimeter

The Compact Muon Solenoid (CMS) [1] detector is a general purpose detector to be installed at the 14 TeV proton-proton collider, LHC, under construction at CERN and due to start operation in 2007. The CMS electromagnetic calorimeter (ECAL) [2] is a hermetic homogeneous calorimeter made of 61,200 scintillating lead tungstate ($PbWO_4$) crystals [3] mounted in the central barrel part, closed by 7,324 crystals in each of the two endcaps. The barrel consists of 36 supermodules, each covering half the barrel length and 20° in azimuth, containing 1700 crystals together with the associated front end electronics.

1.2 Test beam experimental set-up

Test beam data taken in the H4 beam line at CERN in October and November 2004 using electron beams with a range of momenta between 20 and 250 GeV/c, have been used to investigate the performance of the ECAL. A supermodule fully equipped with the final readout electronics [4] was installed on a movable table which allowed the beam to be directed at any part of it. Electrons were incident at an angle of $\simeq 3°$ to the direction of the crystal axis in both transverse directions reproducing the average incident angle of particles emerging from the collision region in LHC running. Plastic scintillator counters were used to trigger the readout. The trigger defines an area of 20×20 mm^2. This area is only slightly smaller than the transverse section of the crystals which have a front section of $\simeq 22 \times 22$ mm^2 and a rear section of $\simeq 25 \times 25$ mm^2. The position of the incident electrons in the transverse directions was determined by four planes of scintillating fibre hodoscopes.

1.3 Readout electronics

The electrical signal from the photodetectors is shaped by a preamplifier and amplified by a multi-gain amplifier (MGPA) before digitization by ADCs at a frequency of 40 MHz [5]. It provides a dynamic range from about 35 MeV to saturation at 1.7 TeV in the barrel. The data read out consists of a series of 10 consecutive digitizations, corresponding to a sequence of samplings of the signal at 40 MHz. The signal amplitude must be reconstructed using these samplings.

2 Reconstruction of the signal amplitude

2.1 The weights method

The method used to reconstruct the amplitude from the digitized samples is based on a digital filtering technique. The signal amplitude, $\hat{\mathcal{A}}$, is computed from a linear combination of discrete time samples (see Equation 1).

$$\hat{\mathcal{A}} = \sum_{i=1}^{N} w_i \times S_i \tag{1}$$

where w_i are the weights, S_i the time sample values in ADC counts and N is the number of samples used in the filtering with the index, i, running over the time samples. The weights w_i are obtained by minimizing the variance of $\hat{\mathcal{A}}$ [6]. When considering the simplest case (no noise correlations between time samples) the optimal weights are given by the formula $w_i = f_i / \sum_{j=1}^{N} f_j^2$, where f_i is the value of the function, $f(t)$, describing the time development of the signal pulse in time, t, at the time t_i of sample i. A form of the function, $f(t)$, that provides a good description of the electronics signal is a digital representation (profile histogram) directly built from the test beam data (see Fig. 1). The determination of the optimum function to be used is addressed in Section 2.3.

Various implementations of the weights method have been tested using test beam data and their ability to reduce the noise contribution is used to discriminate between them.

2.2 Measurement of the electronics noise

In the following, we compare the final electronics noise obtained when implementing a "5-weights" and a "3+5-weights" method. The 5-weights method uses the sample on the peak, the one before and the 3 after while the 3+5-weights also uses the 3 pre-samples (before any signal appears). The first implementation requires the pedestal to

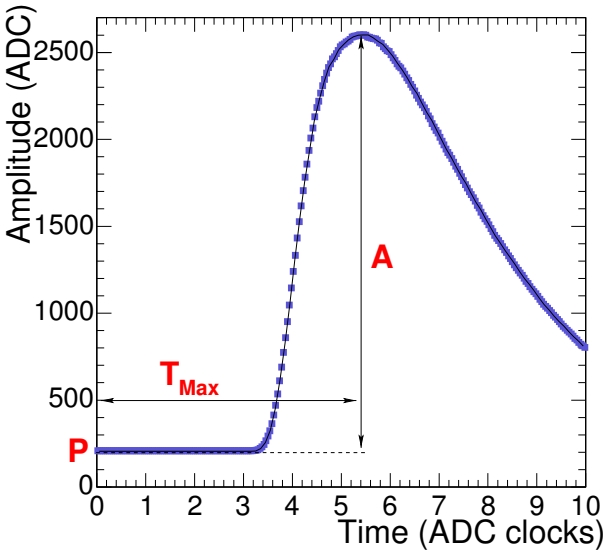

Figure 1: Profile of the signal pulse from a crystal of the supermodule using an electron beam of 120 GeV. The peaking time T_{Max}, the pedestal P and the amplitude of the signal A are shown.

be determined independently and subtracted prior to reconstruction, while the second allows a subtraction of the pedestal on an event by event basis (the so-called "pedestal subtracting weights"). For completeness, a 3+1 weights pedestal-subtracting implementation has also been studied. The single weight is then applied to the sample on the peak. This allows the demonstration of the impact of dynamic baseline subtraction in its simplest form. Table 1 summarizes the ECAL noise measured by examining the variation of the reconstructed amplitude for data taken with random triggers, when no signal is present.

Table 1: Noise in ADC counts measured in a single channel and arrays of 3×3 and 5×5 channels for three different implementations of the amplitude reconstruction method, and for a single sampling. 1 ADC count $\simeq$ 37 MeV.

Method	Noise (ADC counts)		
	1×1	3×3	5×5
Single sampling	1.20±0.01	3.7±0.04	6.5±0.1
5-weights	1.11±0.02	3.8±0.1	6.7±0.1
3+1 Pedestal subtracting weights	1.13±0.03	3.4±0.1	5.7±0.1
3+5 Pedestal subtracting weights	1.07±0.02	3.2±0.1	5.4±0.1

The results given in the table show that the lowest noise is achieved by the pedestal-subtracting weights. This implies the presence of low frequency noise which is removed by the dynamic pedestal subtraction. Comparing the noise seen in a single channel with that seen in sums of 3×3 and 5×5 channels shows a small contribution of noise correlations between channels. This is entirely removed by the use of the pedestal subtracting weights. This implementation is used for reconstructing the signal amplitude. Using five samples in the signal, rather than one, results in a slightly lower value of noise as compared to the 3+1 weights.

2.3 Implementation of the reconstruction method

As mentioned in Section 2.1, the determination of the weights requires knowledge of a signal representation $f(t)$. The impact of the choice of this function on the energy resolution has been studied with test beam data. Two parameters characterize $f(t)$: the signal timing T_{Max} and the parameter C which represents the width of the pulse.

In the test beam the scintillation signals have a random phase with respect to the 25 ns ADC clock interval, while during LHC operation the ADC clock will be synchronous with the bunch crossing. The relevance of the choice of $f(t)$ has been investigated in both cases. To simulate synchronous running, test beam data have been analyzed

taking only events in a single 1 ns bin of phase. Figure 2 shows the energy resolution measured when the weights used to reconstruct the amplitude are derived from signal representations with peaking times and widths which differ from those of the actual signal.

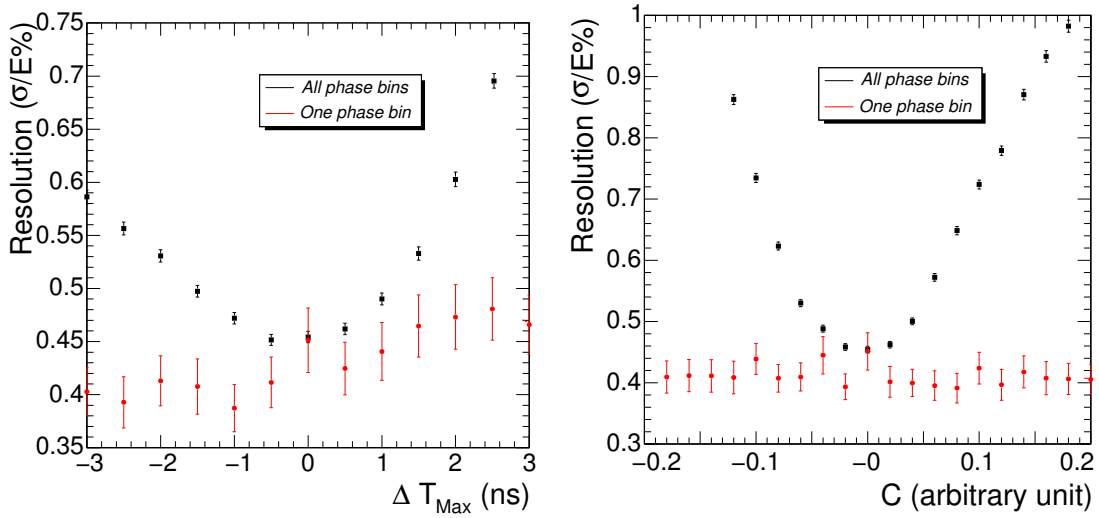

Figure 2: Left: Energy resolution in a 3×3 matrix of crystals measured with a 120 GeV electron beam, as a function of the timing difference (ΔT_{Max}). Right: Energy resolution as a function of the contraction factor, C ($t \rightarrow t + \mathrm{C} \times (t - T_{\mathrm{Max}})$). The black square points correspond to the summing of all bins in phase as in the asynchronous data taking (Test beam). The red dots correspond to the synchronous mode (CMS) which is reproduced by selecting a single 1 ns bin in phase.

These results suggest that, in the case of synchronous running (such as in CMS operation), the same reference signal representation can be used to derive a single set of weights to be used for the signal amplitude reconstruction of all channels. The uniformity of the readout electronics allows this important simplification. Reconstructing the signal pulse amplitude in test beam is sensitive to the individual channel signal timing and shape due to the asynchronous nature of the data taking. When the weights are derived using the signal description specific to each channel, the resolution is as good as the one obtained in a single 1 ns bin.

3 Shower containment variation with position

The energy contained in 3×3 and 5×5 matrices of crystals depends on the particle incidence position on the central crystal. The variation of the energy containment with respect to this position was studied with electron test beam data. A correction based on the balance of energy between crystals can be applied to recover a uniform energy response [7].

3.1 Dependence of the measured energy with the position

Figure 3 displays the reconstructed energy summed in 3×3 and 5×5 arrays of crystals centered on three adjacent crystals, as a function of the η coordinate measured by the hodoscope. The maximum response has been normalized to the beam energy (120 GeV) in each case. The peak to peak variation of the measured energy contained in a matrix decreases from 2.5% for a sum of 9 to 1.6% for a sum of 25 crystals. Similar distributions can be obtained when plotting the energy as a function of ϕ.

3.2 Parametrization of the response with position

The energy balance between crystals can be used to determine the position of incidence. As illustrated by Fig. 4 (left), this method uses the ratio of the energy contained in the side rows (or columns) of crystals to the energy contained in the rest of the matrix (including the central row/column).

Figure 4 (right) shows the energy variation parametrized as a function of position, measured by the variable $\ln(\mathrm{E2/E1})$, using test beam data. In order to better determine this parametrization, data have been recorded

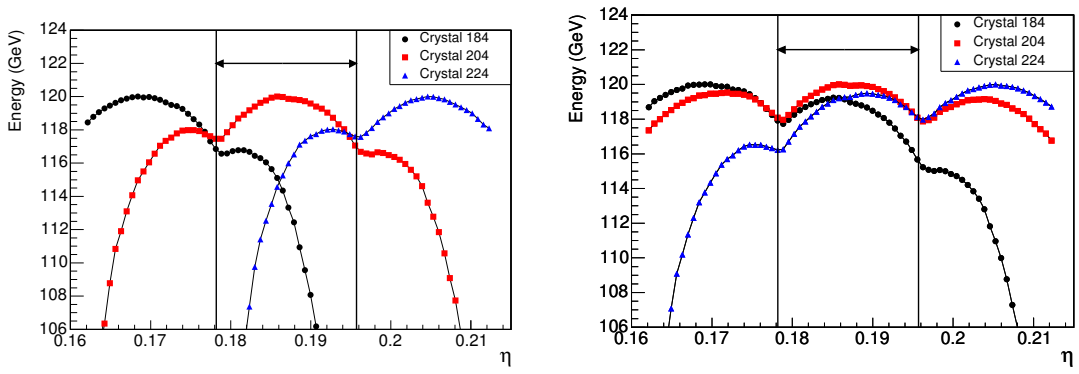

Figure 3: Left: Energy in 3×3 matrices centered on crystals 184 (dots), 204 (squares), 224 (triangles) as a function of η; Right: Same for 5×5 matrices. The double arrow shows the extent of a single crystal.

with the beam directed on the edge of the centre crystal. These functions are used to correct the energy on an event by event basis. An asymmetry can be observed between the distributions in the regions close to the two opposite edges which is due to the 3° off-pointing of the crystals. A single correction function was used for all energies and for all regions in the supermodule.

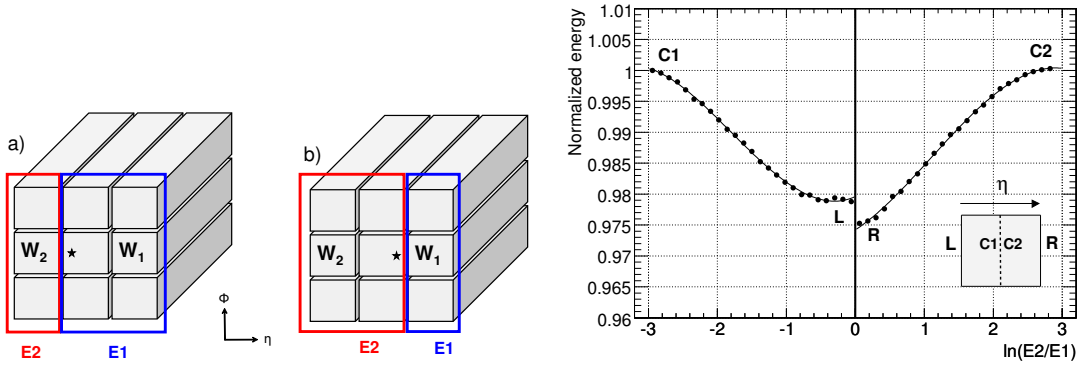

Figure 4: Left: Definition of clustered crystal energy into E1 and E2 in the case where W1<W2 (a) and W1>W2 (b) (W1 and W2 are the energies of the crystals on either side of the centre crystal). Right: Normalized sum of energy measured in 9 crystals versus $\ln(\mathrm{E2/E1})$ in the η views for crystal 204 ($\eta = 0.187$). The crystal 204 has always the maximum energy. The lines are third order polynomial functions fitted to the measured distributions (independently for positive and negative values of $\ln(\mathrm{E2/E1})$ because of the asymmetry mentioned before).

4 Energy resolution

Results on energy resolution are given for both electrons in a small region of incidence and for electrons with uniform incidence over the calorimeter surface. The electron-induced shower energy is reconstructed in matrices of 3×3 crystals centred on the crystal containing the maximum energy. Corrections for variations in the shower containment are applied in the case of uniform incidence.

4.1 Intrinsic energy resolution

As explained in Section 3, the electron shower energy contained in a crystal matrix depends on the shower position. Investigating the energy resolution in the central incidence region, defined as a limited 4×4 mm^2 region around the point of maximum containment, gives a measure of the intrinsic resolution of the calorimeter. In this region, the containment is almost constant.

In the following, results are given for runs with 30 000 events taken in crystal 704, located at pseudorapidity $\eta = 0.62$. The energy spectra for 120 GeV electrons reconstructed in a 3×3 matrix centred on crystal 704 is shown in Fig. 5 (left). The energy scale in these plots is obtained by normalizing the mean signal amplitude to the beam momentum. The crystals were intercalibrated with constants determined directly from the test beam data.

The energy dependence of the resolution is studied for data taken at a series of beam energies: 20, 30, 50, 80, 120, 180 and 250 GeV. The energy dependence is fitted by the following functional form :

$$\left(\frac{\sigma}{E}\right)^2 = \left(\frac{S}{\sqrt{E}}\right)^2 + \left(\frac{N}{E}\right)^2 + C^2 \tag{2}$$

where S is the stochastic term, N the noise and C the constant term (E is in GeV). The fit is performed with the noise term fixed at its measured value. The energy resolution values for a 3×3 matrix centred on crystal 704 is shown in Fig. 5, together with the fitted resolution function.

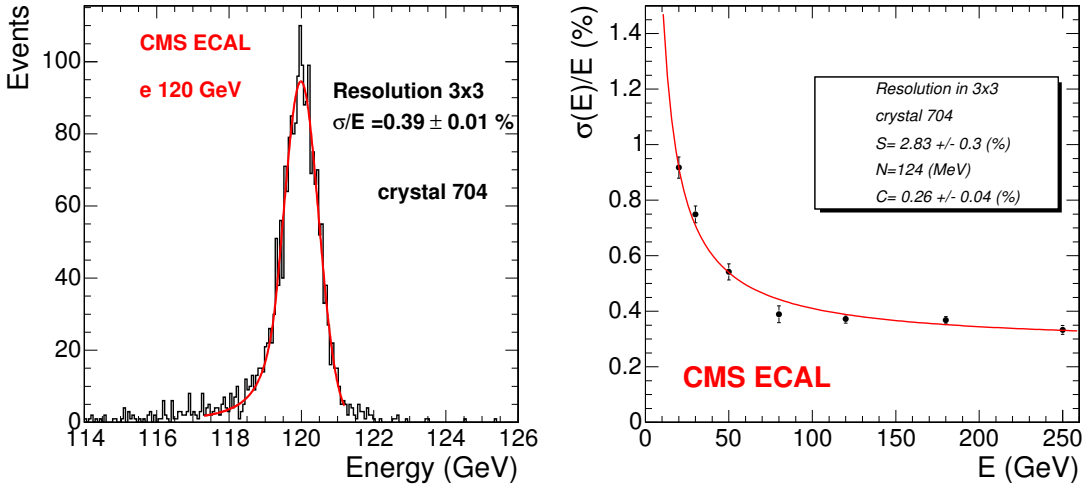

Figure 5: Left: Distribution of energy reconstructed in a 3×3 crystal matrix centered on crystal 704 for electrons at 120 GeV. Right: Resolution as a function of the energy reconstructed by summing for the same matrix after hodoscope cuts of 4×4 mm^2.

4.2 Energy resolution for uniform impact

Figure 6 shows the effect of shower containment corrections summing data from many runs where the incident beam is impacting at many locations on an array of 9 crystals. This configuration reproduces quite well a uniform coverage of an array of 9 crystals. The measured relative resolution at 120 GeV is 0.50%.

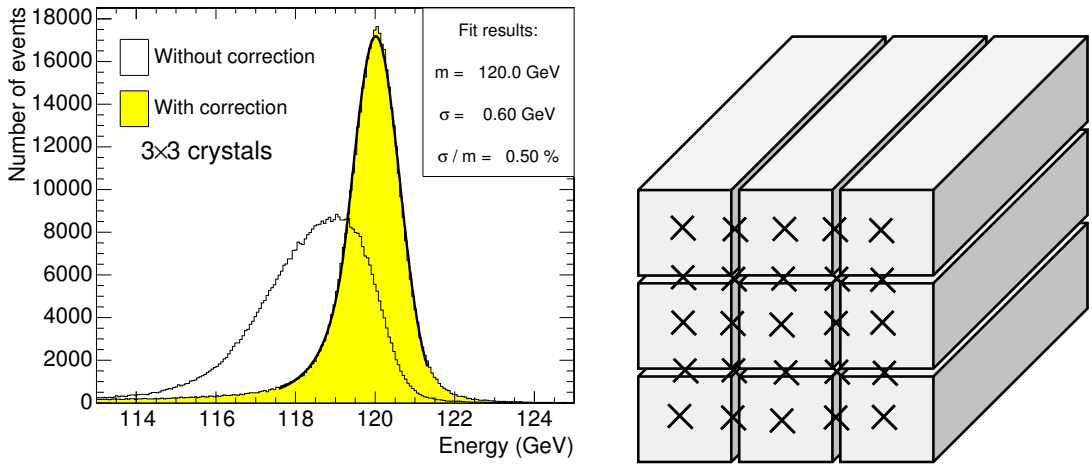

Figure 6: Distribution of energy before (unshaded) and after shower containment corrections (shaded) when the incident beam is centered at many locations of an array of 3×3 crystals as shown by the black crosses on the right side of the Figure.

5 Conclusion

Test beam data taken in 2004 allowed exhaustive performance studies to be made on one CMS ECAL supermodule. Reconstruction of the signal amplitude in the CMS ECAL can be performed by a digital filtering technique. An implementation with dynamic pedestal subtraction gives a noise in a single channel of 40 MeV, and coherent noise between channels is effectively removed. In synchronous running, as will be the case at LHC, a single set of weights can be used to reconstruct the amplitude in all channels.

Consistent energy resolution is obtained for electrons with central incidence in different areas of the calorimeter. The resolution obtained using the energy reconstructed in a matrix of 3×3 crystals is $0.40\pm0.01\%$ for electrons of 120 GeV. A typical energy dependent resolution for central incidence gives a stochastic term of 2.8% and a constant term of 0.3%. For a uniform incidence, shower containment can be effectively corrected to give a resolution better than 0.5% for electrons of energy greater than 100 GeV. The resolution measured for the supermodule is compatible with design expectations.

References

[1] CMS Collaboration, *"The Compact Muon Solenoid Technical Proposal"*, CERN/LHCC 94-38, 1994

[2] CMS Collaboration, *"The Electromagnetic Calorimeter Technical Design Report"*, CERN/LHCC 1997-033, 1997

[3] A.A. Annenkov, P. Lecoq and M.V. Korzhik, *"Lead Tungstate scintillation material"*, Nucl. Instr. and Meth. **A490** (2002) 30

[4] CMS Collaboration, *"CMS Physics Technical Design Report Vol. 1"*, CERN/LHCC 2006-001 (February 2006) 547pp

[5] Raymond, M. *et al.*, *"The MGPA Electromagnetic Calorimeter Readout Chip for CMS"*, Proceedings of the 9th Workshop on Electronics for the LHC Experiments, CERN-LHCC-2003-055, 2003

[6] CMS ECAL Group, *"Reconstruction of the signal amplitude of the CMS electromagnetic calorimeter"*, The European Physical Journal C, Vol 46, Sup 1, 2006, pp:23–35

[7] J. Descamps and P. Jarry, *"Performance of the cluster containment correction for the CMS electromagnetic calorimeter barrel"*, CMS Note 2006/045.